Synchronization in large directed networks of coupled phase oscillators

Juan G. Restrepo[a)]
Institute for Research in Electronics and Applied Physics, University of Maryland, College Park, Maryland 20742 and Department of Mathematics, University of Maryland, College Park, Maryland 20742

Edward Ott
Institute for Research in Electronics and Applied Physics, University of Maryland, College Park, Maryland 20742 and Department of Physics and Department of Electrical and Computer Engineering, University of Maryland, College Park, Maryland 20742

Brian R. Hunt
Department of Mathematics, University of Maryland, College Park, Maryland 20742 and Institute for Physical Science and Technology, University of Maryland, College Park, Maryland 20742

(Received 29 August 2005; accepted 11 November 2005; published online 31 March 2006)

We study the emergence of collective synchronization in large directed networks of heterogeneous oscillators by generalizing the classical Kuramoto model of globally coupled phase oscillators to more realistic networks. We extend recent theoretical approximations describing the transition to synchronization in large undirected networks of coupled phase oscillators to the case of directed networks. We also consider the case of networks with mixed positive-negative coupling strengths. We compare our theory with numerical simulations and find good agreement. © *2005 American Institute of Physics*. [DOI: 10.1063/1.2148388]

Synchronization of coupled oscillators is frequently observed in nature and technology.[1,2] Recently, the study of synchronization phenomena in complex networks has received much attention.[3–12] A classical model for the phase dynamics of weakly coupled oscillators is that of Kuramoto,[13,14] who showed that as the coupling strength is increased there is a transition from incoherent behavior to synchronization. The Kuramoto model assumes all-to-all connectivity and positive coupling (i.e., the coupling of two oscillators tends to reduce their phase difference). However, it has been recently noted that the topology of real world networks is often very complex. In the current paper, generalizing our previous work which considered the case of large undirected coupling networks with positive coupling,[12] we discuss the synchronization of many phase oscillators interacting on large directed networks with mixed positive/negative coupling.

I. INTRODUCTION

The classical Kuramoto model[13,14] describes a collection of globally coupled phase oscillators that exhibits a transition from incoherence to synchronization as the coupling strength is increased past a critical value. Since real world networks typically have a more complex structure than all-to-all coupling,[15,16] it is natural to ask what effect interaction structure has on the synchronization transition. In Ref. 12, we studied the Kuramoto model allowing general connectivity of the nodes, and found that for a large class of networks there is still a transition to global synchrony as the coupling strength exceeds a critical value k_c. We found that the critical coupling strength depends on the largest eigenvalue of the adjacency matrix A describing the network connectivity. We also developed several approximations describing the behavior of an order parameter measuring the coherence past the transition. This past work was restricted to the case in which $A_{nm}=A_{mn}\geqslant 0$, that is, undirected networks in which the coupling tends to reduce the phase difference of the oscillators.

Most networks considered in applications are directed,[15,16] which implies an asymmetric adjacency matrix, $A_{nm}\neq A_{mn}$. Also, in some cases the coupling between two oscillators might drive them to be out of phase, which can be represented by allowing the coupling term between these oscillators to be negative, $A_{nm}<0$. The effect that the presence of directed and mixed positive-negative connections can have on synchronization is, therefore, of interest. Here we show how our previous theory can be generalized to account for these two factors. We study examples in which either the asymmetry of the adjacency matrix or the effect of the negative connections are particularly severe and compare our theoretical approximations with numerical solutions.

This paper is organized as follows. In Sec. II we review the results of Ref. 12 for undirected networks with positive coupling. In Sec. III we consider directed networks, and in Sec. IV we study networks with mixed positive-negative coupling. In Sec. V we present examples and comparisons of our theory with numerical simulations. In Sec. VI we discuss our results. In the Appendix we discuss the spectrum of certain matrices used in our examples.

II. BACKGROUND

In this section we will review previous results for undirected networks with positive coupling. In Ref. 12 we considered the onset of synchronization in large networks of

a)Electronic mail: juanga@math.umd.edu

many heterogeneous coupled phase oscillators. This situation can be modeled by the equation

$$\dot{\theta}_n = \omega_n + k\sum_{m=1}^{N} A_{nm}\sin(\theta_m - \theta_n), \tag{1}$$

where θ_n, ω_n are the phase and natural frequency of oscillator n, and $N \gg 1$ is the total number of oscillators. The frequencies ω_n are assumed to be independently drawn from a probability distribution characterized by a density function $g(\omega)$ that is symmetric about a single local maximum at $\omega = \bar{\omega}$. The mean frequency $\bar{\omega}$ can be shifted to $\bar{\omega}=0$ by introduction of the change of variables $\theta_n \to \theta_n - \bar{\omega}t$. Thus we henceforth take $\bar{\omega}=0$. The adjacency matrix $\{A_{nm}\}$ determines the network connecting the oscillators. Positive coupling was imposed in Ref. 12 by the condition $A_{nm} \geqslant 0$. Furthermore, the matrix A was assumed to be symmetric and thus only undirected networks were considered. In this section we will review our results for this class of networks, following Sec. II of Ref. 12. Thus throughout this section $A_{nm}=A_{mn} \geqslant 0$.

In order to quantify the coherence of the inputs to a given node, a positive real valued local order parameter r_n is defined by

$$r_n e^{i\psi_n} \equiv \sum_{m=1}^{N} A_{nm}\langle e^{i\theta_m}\rangle_t, \tag{2}$$

where $\langle\cdots\rangle_t$ denotes a time average. To characterize the macroscopic coherence for the whole network, a global order parameter is defined by

$$r = \frac{\sum_{n=1}^{N} r_n}{\sum_{n=1}^{N} d_n}, \tag{3}$$

where d_n is the degree of node n defined by

$$d_n = \sum_{m=1}^{N} A_{nm}. \tag{4}$$

In terms of r_n, Eq. (1) can be rewritten as

$$\dot{\theta}_n = \omega_n - kr_n\sin(\theta_n - \psi_n) - kh_n(t), \tag{5}$$

where the term $h_n(t)$ takes into account time fluctuations and is given by $h_n = \mathrm{Im}\{e^{-i\theta_n}\Sigma_m A_{nm}(\langle e^{i\theta_m}\rangle_t - e^{i\theta_m})\}$, where Im stands for the imaginary part. Assuming the terms in this sum to be statistically independent, we expect $h_n(t)$ to be of order $(\Sigma_m A_{nm}^2)^{1/2}$, which is proportional to the square root of the number of connections of node n. Past the transition to coherence, r_n should be proportional to d_n, which is in turn proportional to the number of connections of node n. Thus if the number of connections per node is large, h_n will be small compared to r_n except very close to the transition, where $r_n \to 0$. We, therefore, expect our approximations to work better sufficiently above the transition to coherence. (At the transition we expect, as in the classical Kuramoto problem, the fluctuations to be the dominant term.) Henceforth, we will assume that the number of connections into each node is large enough that we can neglect the time fluctuations represented by the term h_n, obtaining from Eq. (5)

$$\dot{\theta}_n = \omega_n - kr_n\sin(\theta_n - \psi_n). \tag{6}$$

We have found numerically that the effect of a significant fraction of the nodes having few connections is to shift the transition to coherence to higher values of the coupling constant. The amount of shift in the critical coupling constant can be estimated by treating the time fluctuations $h_n(t)$ as a noise term. For a more detailed discussion, see Sec. VI of Ref. 12.

From Eq. (6), we conclude that oscillators with $|\omega_n| \leqslant kr_n$ become locked, i.e., for these oscillators θ_n settles at a value for which

$$\sin(\theta_n - \psi_n) = \omega_n/(kr_n). \tag{7}$$

Then

$$r_n = \sum_{|\omega_m|\leqslant kr_m} A_{nm}e^{i(\theta_m-\psi_n)} + \sum_{|\omega_m|>kr_m} A_{nm}\langle e^{i(\theta_m-\psi_n)}\rangle_t. \tag{8}$$

The sum over the nonlocked oscillators can be shown to vanish in the large number of connections per node limit (see Appendix A of Ref. 12), and we obtain from the real and imaginary parts of Eq. (8)

$$r_n = \sum_{|\omega_m|\leqslant kr_m} A_{nm}\cos(\psi_m - \psi_n)\sqrt{1-\left(\frac{\omega_m}{kr_m}\right)^2} - \sum_{|\omega_m|\leqslant kr_m} A_{nm}\sin(\psi_m - \psi_n)\left(\frac{\omega_m}{kr_m}\right) \tag{9}$$

and

$$0 = \sum_{|\omega_m|\leqslant kr_m} A_{nm}\cos(\psi_m - \psi_n)\left(\frac{\omega_m}{kr_m}\right) + \sum_{|\omega_m|\leqslant kr_m} A_{nm}\sin(\psi_m - \psi_n)\sqrt{1-\left(\frac{\omega_m}{kr_m}\right)^2}. \tag{10}$$

Introducing the assumption that the solutions ψ_n, r_n are statistically independent of ω_n (as in Ref. 12) and using the assumed symmetry of the frequency distribution $g(\omega)$ we obtain from Eq. (9) the approximation,

$$r_n = \sum_{|\omega_m|\leqslant kr_m} A_{nm}\cos(\psi_m - \psi_n)\sqrt{1-\left(\frac{\omega_m}{kr_m}\right)^2}, \tag{11}$$

and the right side of Eq. (10) is approximately zero for large number of connections per node. The solution of Eq. (11) with $\psi_n=\psi_m$ for all n is the one corresponding to the smallest value of k, and thus corresponds to the smallest critical coupling k_c leading to a transition to a macroscopic value of r_n. Therefore, we consider the equation

$$r_n = \sum_{|\omega_m|\leqslant kr_m} A_{nm}\sqrt{1-\left(\frac{\omega_m}{kr_m}\right)^2}. \tag{12}$$

We refer to this approximation [Eq. (12)], based on neglecting the time fluctuations, as the *time averaged theory* (TAT). In Ref. 12 we showed numerically that this approximation consistently describes the large time behavior of the order parameter r past the transition for various undirected networks with positive coupling strengths (i.e., $A_{nm}=A_{mn} \geqslant 0$).

Averaging over the frequencies, one obtains the *frequency distribution approximation* (FDA)

$$r_n = k\sum_m A_{nm} r_m \int_{-1}^{1} g(zkr_m)\sqrt{1-z^2}dz. \tag{13}$$

The value of the critical coupling strength can be obtained from the frequency distribution approximation by letting $r_n \to 0^+$, producing

$$r_n^{(0)} = \frac{k}{k_0}\sum_m A_{nm} r_m^{(0)}, \tag{14}$$

where $k_0 \equiv 2/[\pi g(0)]$. The critical coupling strength thus corresponds to

$$k_c = \frac{k_0}{\lambda}, \tag{15}$$

where λ is the largest eigenvalue of the adjacency matrix A and $r^{(0)}$ is proportional to the corresponding eigenvector of A. By considering perturbations from the critical values as $r_n = r_n^{(0)} + \delta r_n$, expanding $g(zkr_m)$ in Eq. (13) to second order for small argument, multiplying Eq. (13) by $r_n^{(0)}$ and summing over n, we obtained an expression for the order parameter past the transition valid for networks with relatively homogeneous degree distributions[17]

$$r^2 = \left(\frac{\eta_1}{\alpha k_0^2}\right)\left(\frac{k}{k_c}-1\right)\left(\frac{k}{k_c}\right)^{-3}, \tag{16}$$

for $0 < (k/k_c) - 1 \ll 1$, where

$$\eta_1 \equiv \frac{\langle u\rangle^2 \lambda^2}{N\langle d\rangle^2 \langle u^4\rangle}, \tag{17}$$

$\alpha = -\pi g''(0) k_0/16$, u is the normalized eigenvector of A corresponding to λ, and $\langle\cdots\rangle$ is defined by $\langle x^q\rangle = \Sigma_{n=1}^N x_n^q/N$.

The *mean field theory* (MFT)[9,10] was obtained from the frequency distribution equation by introducing the extra assumption that the local mean field is approximately proportional to the degree, $r_n = r d_n$. Substituting this into Eq. (13) and summing over n we obtained

$$\sum_{m=1}^{N} d_m = k\sum_{m=1}^{N} d_m^2 \int_{-1}^{1} g(zkrd_m)\sqrt{1-z^2}dz. \tag{18}$$

Letting $r \to 0^+$, the critical coupling strength is given by

$$k \equiv k_{mf} = k_0 \frac{\langle d\rangle}{\langle d^2\rangle}. \tag{19}$$

An expansion to second order yields

$$r^2 = \left(\frac{\eta_2}{\alpha k_0^2}\right)\left(\frac{k}{k_{mf}}-1\right)\left(\frac{k}{k_{mf}}\right)^{-3}, \tag{20}$$

for $0 < (k/k_{mf}) - 1 \ll 1$, where

$$\eta_2 \equiv \frac{\langle d^2\rangle^3}{\langle d^4\rangle\langle d\rangle^2}. \tag{21}$$

Comparing the above three approximations, we note the following points:

(1) The TAT requires knowledge of the adjacency matrix and the particular realization of the oscillator frequencies ω_n at each node;
(2) the FDA requires knowledge of the adjacency matrix and the frequency distribution, but averages over realizations of the node frequencies;
(3) the MFT (like the FDA) averages over realizations of the node frequencies, but only requires knowledge of the degree distribution d_m (knowledge of the adjacency matrix is not required);
(4) computationally, the TAT and the FDA are more demanding than the MFT; all three, however, are much less costly than direct integration of Eq. (1) to find the time asymptotic result;
(5) finally, one might suspect that the TAT is more accurate for describing a specific system realization, given that one has knowledge of the network and the realization of the oscillator frequencies ω_n on each node, while the FDA might be more appropriate for investigating the mean behavior averaged over an ensemble of realizations of the oscillator frequencies.

The approach here is to look at a coupling strength small enough so that there is an incoherent state; then we increase the coupling strength until a coherent synchronized behavior emerges, and we then follow this coherent attractor continuously to larger values of the coupling parameter. We note that this consideration does not address the issue of the possibility of other coexisting attractors that may be present in addition to those we consider.

III. DIRECTED NETWORKS

In this section we will extend our previous results to include directed networks, $A_{nm} \neq A_{mn}$. As in the previous section, we will assume that the number of connections per node (both incoming and outgoing) is large, that the frequencies are drawn randomly from a distribution symmetric around its unique local maximum at $\omega = 0$, and that the coupling is positive, $A_{nm} \geqslant 0$. We define the *in-degree* d_n^{in} and *out-degree* d_n^{out} of node n as

$$d_n^{\text{in}} \equiv \sum_{m=1}^{N} A_{nm} \tag{22}$$

and

$$d_n^{\text{out}} \equiv \sum_{m=1}^{N} A_{mn}. \tag{23}$$

For directed networks, the degrees d_n^{in} and d_n^{out} may be unequal, and it is, therefore, necessary to take this difference into account when developing approximations for the synchronization transition based on the degree of the nodes [e.g., the mean-field theory, Eq. (18)].

The approximations to r given by the time averaged theory [Eq. (12)], the frequency distribution approximation [Eq. (13)], and the estimate for the critical coupling constant given by Eq. (15) are still valid in this more general case. The existence of a non-negative real eigenvalue λ larger than

the magnitude of any other eigenvalue is guaranteed for matrices with non-negative entries by the Frobenius theorem,[18] and we use this eigenvalue in Eq. (15).

We now consider the perturbation solution to the FDA [Eq. (13)] for $(k-k_c)$ small taking into account asymmetry of A. Expanding Eq. (13) to second order in kr_n, inserting $r_n = r_n^{(0)} + \delta r_n$, and canceling terms of order $r_n^{(0)}$, the leading order terms remaining are

$$\delta r_n = \frac{k}{k_c\lambda}\sum_m A_{nm}\delta r_m - \frac{\alpha k^3}{k_c\lambda}\sum_m A_{nm}(r_m^{(0)})^3 + \frac{k-k_c}{k_c\lambda}\sum_m A_{nm} r_m^{(0)}. \tag{24}$$

In order for Eq. (24) to have a solution for δr_n, it must satisfy a solubility condition. This condition can be obtained as follows. Let $\bar{u}_n$ be an eigenvector of the transpose of A, A^T, with eigenvalue λ. Multiplying Eq. (24) by $\bar{u}_n$, summing over n and using Eq. (14), we obtain

$$\frac{\sum_m (r_m^{(0)})^3 \bar{u}_m}{\sum_m r_m^{(0)}\bar{u}_m} = \frac{k-k_c}{\alpha k^3}. \tag{25}$$

In terms of u and $\bar{u}$, eigenvectors of A and A^T associated with the eigenvalue λ, the square of the order parameter r can be expressed as [cf. Eqs. (16) and (17)]

$$r^2 = \left(\frac{\bar{\eta}_1}{\alpha k_0^2}\right)\left(\frac{k}{k_c}-1\right)\left(\frac{k}{k_c}\right)^{-3}, \tag{26}$$

for $0 < (k/k_c) - 1 \ll 1$, where

$$\bar{\eta}_1 \equiv \frac{\langle u\rangle^2\langle u\bar{u}\rangle\lambda^2}{N\langle d\rangle^2\langle u^3\bar{u}\rangle}, \tag{27}$$

and $\langle x^p y^q\rangle$ is defined by $\langle x^p y^q\rangle = \Sigma_{n=1}^N x_n^p y_n^q / N$. We will refer to this generalization of the perturbation theory as the *directed perturbation theory* (DPT).

The mean field theory can also be generalized for directed networks by introducing the assumption $r_n = r d_n^{\text{in}}$. We obtain as a generalization of Eq. (18) the *directed mean field theory* (DMFT)

$$\sum_{m=1}^N d_m^{\text{in}} = k\sum_{m=1}^N d_m^{\text{in}} d_m^{\text{out}} \int_{-1}^1 g(zkrd_m^{\text{in}})\sqrt{1-z^2}\,dz. \tag{28}$$

Letting $r \to 0^+$, the critical coupling strength is given by

$$k \equiv k_{mf} = k_0 \frac{\langle d^{\text{in}}\rangle}{\langle d^{\text{in}} d^{\text{out}}\rangle}. \tag{29}$$

An expansion to second order yields [cf. Eqs. (20) and (21)]

$$r^2 = \left(\frac{\bar{\eta}_2}{\alpha k_0^2}\right)\left(\frac{k}{k_{mf}}-1\right)\left(\frac{k}{k_{mf}}\right)^{-3}, \tag{30}$$

for $0 < (k/k_{mf}) - 1 \ll 1$, where

$$\bar{\eta}_2 \equiv \frac{\langle d^{\text{in}} d^{\text{out}}\rangle^3}{\langle (d^{\text{in}})^3 d^{\text{out}}\rangle\langle d^{\text{in}}\rangle^2}. \tag{31}$$

IV. NETWORKS WITH NEGATIVE COUPLING

Here we extend our previous results to the case in which the matrix elements A_{nm} are allowed to be negative. In this case, a solution to Eqs. (9) and (10) in which all the phases are equal, $(\psi_n = \psi_m$ for all $n, m)$, does not necessarily exist. [In fact, if one were to set $\psi_n = \psi_m$ in Eq. (11) the right hand side of Eq. (12) could be negative, while by definition r_n is nonnegative.]

Although in this section we will assume $k \geqslant 0$, the case $k < 0$ can be treated by redefining $k \to -k$ and $A_{nm} \to -A_{nm}$. By neglecting the contribution of the drifting oscillators, using the symmetry of $g(\omega)$ and the assumed independence of ψ_n and r_n from ω_n, we obtain from Eqs. (2), (7), and (8) the equation

$$r_n e^{i\psi_n} = \sum_{|\omega_m| \leqslant kr_m} A_{nm} e^{i\psi_m}\sqrt{1-\left(\frac{\omega_m}{kr_m}\right)^2}. \tag{32}$$

Our approach will now be to solve Eq. (32) numerically for ψ_n and r_n. We note that such numerical solution will still be orders of magnitude faster than finding the exact temporal evolution of the network by numerically integrating Eqs. (1). In order to numerically solve Eq. (32) for the variables ψ_n, r_n, we look for fixed points of the following mapping, $(r_n^j, \psi_n^j) \to (r_n^{j+1}, \psi_n^{j+1})$, defined by

$$r_n^{j+1} e^{i\psi_n^{j+1}} = \sum_{|\omega_m| \leqslant kr_m^j} A_{nm} e^{i\psi_m^j}\sqrt{1-\left(\frac{\omega_m}{kr_m^j}\right)^2}. \tag{33}$$

Repeatedly iterating the above map starting from random initial conditions, the desired solution will be produced if the orbit converges to a fixed point. We will discuss the convergence of this procedure when considering particular examples.

We now comment on some aspects introduced by connections with negative coupling. First, we note that when the coupling between the oscillators is positive, the effect of the coupling between them is a tendency to reduce their phase difference. In this case, as $k \to \infty$, the phases synchronize, $\theta_n \to 0$. There is in this case frequency and phase synchronization [i.e., $(d/dt)(\theta_n - \theta_m) \to 0$ and $(\theta_n - \theta_m) \to 0$]. On the other hand, two oscillators coupled with a negative connection $A_{nm} < 0$ tend to oscillate out of phase. However, in a network with many nodes and mixed positive-negative connections, the relative phases of two oscillators cannot in general be determined only from the sign of their coupling. When the oscillators lock, their relative phase is determined by ψ_n [let $k \to \infty$ in Eq. (7)], and in general the phases ψ_n can be broadly distributed in $[0, 2\pi)$. Therefore, in this case we expect frequency synchronization, but not phase synchronization [i.e., $(d/dt)(\theta_n - \theta_m) \to 0$ but $(\theta_n - \theta_m) \nrightarrow 0$]. We also note that in this case the order parameter r, as we have defined it in Eq. (3), may attain values higher than 1 for $k \to \infty$. We, therefore, replace the definition (3) by

$$r = \frac{\sum_{n=1}^{N} r_n}{\sum_{m=1}^{N}\sum_{n=1}^{N} |A_{nm}|}. \tag{34}$$

Note that if $A_{nm} \geqslant 0$ this definition reduces to the previous one.

From Eq. (11) we have for $k \to \infty$

$$r \to \frac{\sum_{m,n} A_{nm} \cos(\psi_m - \psi_n)}{\sum_{m,n} |A_{nm}|}. \tag{35}$$

The order parameter achieves its maximum value, $r=1$, when the phase difference $\psi_m - \psi_n$ between two oscillators is 0 for positive coupling ($A_{nm} > 0$) and π for negative coupling ($A_{nm} < 0$). An order parameter smaller than 1 as $k \to \infty$ indicates frustration in the collection of coupled oscillators, i.e., the phase difference favored by the coupling between each pair of oscillators cannot be satisfied simultaneously by all pairs.[19] The order parameter is similar to the overlap function used in neural networks for measuring the closeness of the state of the network to a memorized pattern.[20]

Using the assumption that the number of connections per node is large, we average Eq. (32) over the frequencies to obtain the approximation

$$r_n e^{i\psi_n} = k \sum_{m=1}^{N} A_{nm} e^{i\psi_m} r_m \int_{-1}^{1} \sqrt{1-z^2}\, g(zkr_m)\, dz. \tag{36}$$

The critical coupling strength k_c can be estimated by letting $r_n \to 0^+$ to be as in Sec. II

$$k_c = \frac{k_0}{\lambda}, \tag{37}$$

where $k_0 = 2/[\pi g(0)]$ and we have assumed the existence of a positive real eigenvalue λ which is larger than the real part of all other (possibly complex) eigenvalues of A. We now discuss the validity of this assumption.

If the adjacency matrix A is asymmetric and there are mixed positive-negative connections (both $A_{nm} > 0$ and $A_{n'm'} < 0$ for some n, m, n', m'), it might occur that the matrix A has no real eigenvalues, or it has complex eigenvalues with real part larger than the largest real eigenvalue. In our examples we find, however, that when there is a bias towards positive coupling strengths, there is a real eigenvalue λ with real part larger than that of the other eigenvalues. Furthermore, the largest real part of the remaining eigenvalues is typically well separated from λ. This issue is discussed further and illustrated with the spectrum of a particular matrix in the Appendix .

So far, we have considered situations in which coupling from oscillator m to oscillator n favors a phase difference $\theta_n - \theta_m = 0$ (positive coupling, $A_{nm} > 0$), or situations in which a phase difference $\theta_n - \theta_m = \pi$ is favored (negative coupling, $A_{nm} < 0$). A more general case is that in which coupling from oscillator m to oscillator n favors a phase difference $\theta_n - \theta_m = \alpha_{nm}$, with $0 \leqslant \alpha_{nm} < 2\pi$. (Such nontrivial phase differences could be favored, for example, by a time delay in the interaction of the oscillators in conditions in which, in the absence of a delay, their interaction would reduce their phase difference to zero.) This more general case can be described by the following generalization of Eq. (1):

$$\dot{\theta}_n = \omega_n + k \sum_{m=1}^{N} |A_{nm}| \sin(\theta_m - \theta_n + \alpha_{nm}). \tag{38}$$

In this scenario, positive coupling corresponds to $\alpha_{nm} = 0$ and negative coupling to $\alpha_{nm} = \pi$. By considering complex values of the coupling constants

$$A_{nm} = |A_{nm}| e^{i\alpha_{nm}}, \tag{39}$$

the same process described at the beginning of this section can be used to show that Eq. (32) is still valid in this more general case. For simplicity, in our examples we will consider cases in which α_{nm} is either 0 or π.

V. EXAMPLES

In this section we will numerically test our approximations (Secs. III and IV) with examples.

In Ref. 12 we showed how our theory described the behavior of the order parameter r for a particular realization of the network and the frequencies. Although the agreement was very good, there was a small but noticeable difference between the time averaged theory and the frequency distribution approximation. Here, besides the asymmetry of the adjacency matrix, we will investigate the variations that occur when different realizations of the network and the frequencies of the individual oscillators are considered. We will show that the small discrepancies mentioned above can be accounted for by averaging over many realizations of the frequencies.

We will compare the approximations described in this section with the numerical solution of Eq. (1) for different types of networks. When numerically solving Eq. (1), the initial conditions for θ_n are chosen randomly in the interval $[0, 2\pi)$ and Eq. (1) is integrated forward in time until a stationary state is reached (stationary state here means stationary in a statistical sense; i.e., although the solution might be time dependent, its statistical properties remain constant in time). From the values of $\theta_n(t)$ obtained for a given k, the order parameter r is estimated using Eqs. (2) and (3), where the time average is taken after the system reaches the stationary state. (Close to the transition, the time needed to reach the stationary state is very long, so that it is difficult to estimate the real value of r. This problem also exists in the classical Kuramoto all-to-all model.) The value of k is then increased and the system is allowed to relax to a stationary state, and the process is repeated for increasing values of k. Throughout this section, the frequency distribution is taken to be $g(\omega) = \frac{3}{4}(1-\omega^2)$ for $|\omega| \leqslant 1$ and 0 otherwise.

A. Example (i), a randomly asymmetric network with $A_{nm} > 0$

As our first example [example (i)] we consider a directed random network generated as follows. Starting with $N \gg 1$ nodes, we consider all possible ordered pairs of nodes (n, m) with $n \neq m$ and add a directed link from node n to node m with probability s. (Equivalently, each nondiagonal entry of

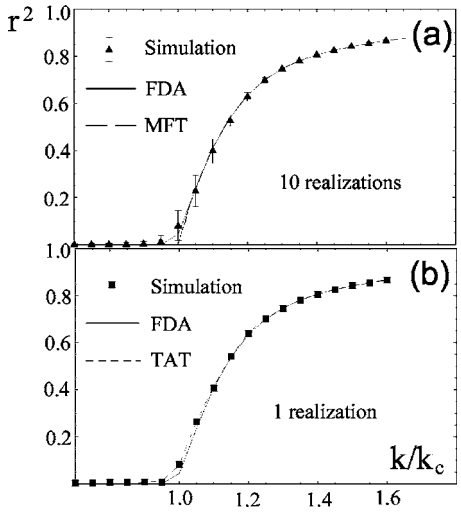

FIG. 1. (a) Average of the order parameter r^2 obtained from numerical solution of Eq. (1) over ten realizations of the network and frequencies (triangles), from the frequency distribution approximation (solid line) and from the directed mean-field theory (long dashed line) as a function of k/k_c. (b) Order parameter r^2 obtained from numerical solution of Eq. (1) for a particular realization of the network and frequencies (boxes), from the time averaged theory (short dashed line) and from the frequency distribution approximation (solid line) as a function of k/k_c.

the adjacency matrix is independently chosen to be 1 with probability s and 0 with probability $1-s$, and the diagonal elements are set to zero.) Even though the network constructed in this way is directed, for most nodes $d_n^{\text{in}} \approx d_n^{\text{out}}$. For $N=1500$ and $s=2/15$, Fig. 1(a) shows the average of the order parameter r^2 obtained from numerical solution of Eq. (1) averaged over ten realizations of the network and frequencies (triangles), the frequency distribution approximation (FDA, solid line), and the mean field theory (MFT, long dashed line) as a function of k/k_c, where the results for the FDA and the MFT are averaged over the ten network realizations (note, however, that the FDA and the MFT do not depend on the frequency realizations). (The perturbation theory Eq. (16) agreed with the frequency distribution approximation and was left out for clarity.) The error bars correspond to one standard deviation of the sample of ten realizations. We note that the larger error bars occur after the transition. When the values of the order parameter are averaged over ten realizations of the network and the frequencies, the results show very good agreement with the frequency distribution approximation and the directed mean field theory.

In order to study how well our theory describes single realizations, we show in Fig. 1(b) the order parameter r^2 obtained from numerical solution of Eq. (1) for a particular realization of the network and frequencies (boxes), the time averaged theory (short dashed line), and the frequency distribution approximation (solid line) as a function of k/k_c. As can be observed from the figure, in contrast with the time averaged theory, the frequency distribution approximation deviates from the numerical solution (boxes) by a small but noticeable amount. This behavior is observed for the other realizations as well. We note that the FDA and MFT results are virtually identical for all ten realizations. On the other hand, the TAT and the results from direct numerical solution of Eq. (1) show dependence on the realization. Since the FDA and MFT incorporate the realizations of the connections A_{nm}, but not the frequencies, we interpret the observed realization dependence of the TAT and the direct solutions of Eq. (1) as indicating that the latter dependence is due primarily to fluctuations in the realizations of the frequencies rather than to fluctuations in the realizations of A_{nm}.

Note that for our example $N=1500$ and $s=2/15$ implies that on average we have $d^{\text{in}} \approx d^{\text{out}} \approx 200$. Thus for comparison purposes, we generated an undirected network as follows: Starting with $N=1500$ nodes, we join pairs of nodes with undirected links in such a way that all nodes have $d_n^{\text{in}} = d_n^{\text{out}} = 200$. This is accomplished by using the configuration model described in Sec. IV of Ref. 15. The resulting network is described by a symmetric adjacency matrix A. The results for this network are similar to those shown in the previous example. This suggests that the asymmetric network in the previous example can be considered (in a statistical sense) as symmetric.

In summary, for the random asymmetric network in example (i) and for the symmetric network described in the previous paragraph (not shown), all the approximations work satisfactorily: Single realizations are described by the time averaged theory, and the average over many realizations is described by the frequency distribution approximation or the directed mean field theory.

B. Example (ii), a strongly asymmetric network with $A_{nm}>0$

Now we consider a network in which the asymmetry has a more pronounced effect [example (ii)]. We consider directed networks defined in the following way. Using the configuration model as above, we first randomly generate an undirected network with $N=1500$ nodes and 400 connections to each node, obtaining a symmetric adjacency matrix A' with entries 0 or 1. We construct directed networks from this undirected network as follows. From the symmetric matrix A', 1's above the diagonal are independently converted into 0's with probability $1-p$, generating by this process an asymmetric adjacency matrix A. (Imagining that the nodes are arranged in order of ascending n along a line, connections pointing in the direction of increasing n are randomly removed. This could model, for example, oscillators which are coupled chemically along the flow of some medium, or flashing fireflies that are looking mostly in one direction.) We will consider a rather low value of p, $p=0.1$, in order to obtain a network with a strong asymmetry.

In Fig. 2 we compare our approximations against the values of the order parameter obtained from numerical solution of Eq. (1) as a function of k/k_c for a network constructed as described above where k_c is given by Eq. (15). In Fig. 2(a) we show the average of the order parameter r^2 [defined by Eq. (3)] versus k/k_c obtained from numerical solution of Eq. (1) over ten realizations of the network and frequencies (triangles), the frequency distribution approximation (solid line), the directed mean field theory Eq. (28) (long dashed line) and the directed perturbation theory Eq. (26) (dot-dashed line). The frequency distribution approximation cap-

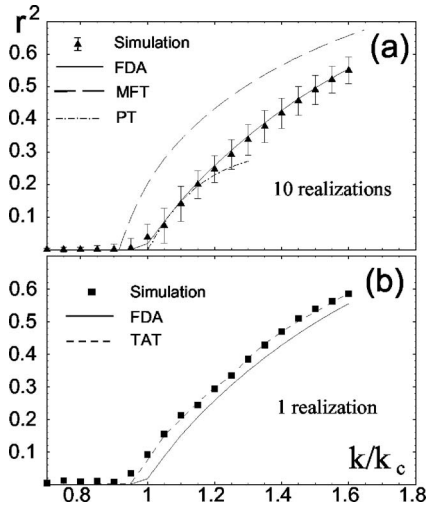

FIG. 2. (a) Average of the order parameter r^2 obtained from numerical solution of Eq. (1) over ten realizations of the network and frequencies with $p=0.1$ (triangles), from the frequency distribution approximation (solid line), from the directed mean field theory (long dashed line), and from the directed perturbation theory (dot-dashed line) as a function of k/k_c. (b) Order parameter r^2 obtained from numerical solution of Eq. (1) for a particular realization of the network and frequencies (boxes), from the time averaged theory (short dashed line) and from the frequency distribution approximation (solid line) as a function of k/k_c.

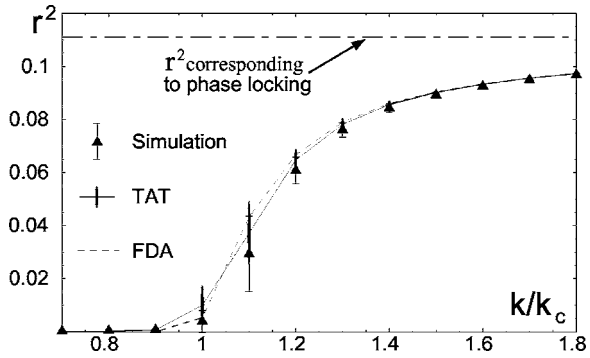

FIG. 3. Average of the order parameter r^2 obtained from numerical solution of Eq. (1) over ten realizations of the network with $q=2/3$ and frequencies (triangles with thin error bars), average of the time averaged theory (solid line with oval error bars), and frequency distribution approximation (dashed line) as a function of k/k_c. The horizontal line represents the value of the order parameter if the oscillators were phase locked ($\theta_n=\theta_m$ for all m and n).

tures, as in the undirected case, the values of the average of the order parameter obtained from numerical solution of Eq. (1). The directed perturbation theory gives a good approximation for small values of k close to k_c, as expected. On the other hand, the directed mean field theory predicts a transition point which is smaller than the one actually observed. We note that for this network solutions of Eq. (1) yield substantial rms deviation of individual realizations [the error bars in Fig. 2(a)] for all $k>k_c$.

Now we consider a single realization. In Fig. 2(b) we show the order parameter r^2 obtained from numerical solution of Eq. (1) for a particular realization of the network and frequencies (boxes), the time averaged theory (short dashed line) and the frequency distribution approximation (solid line) as a function of k/k_c. The time averaged theory tracks the value of the order parameter for this particular realization. This is also observed for the other realizations.

As an indication of why the directed mean-field theory gives a smaller transition point than that given by k_c in Eq. (15), we note that in the limiting case, $p\to 0$, all the elements above and in the diagonal of A are 0, so that $\lambda=0$ and $k_c\to\infty$. However, the directed mean field theory predicts a transition at the finite value $k_{mf}=k_0\langle d^{\text{in}}\rangle/(\langle d^{\text{in}}d^{\text{out}}\rangle)$.

C. Examples of networks with negative coupling

Now we consider examples in which there are negative connections, i.e., some of the entries of the adjacency matrix are negative, $A_{nm}<0$. In our next example, we construct first an undirected network with $N=1500$ nodes and 400 connections per node. We then set $A_{nm}=0$ if n and m are not connected, and if they are we set A_{nm} to 1 with probability q and to -1 with probability $1-q$.

First we consider the case $q=2/3$, so that one-third of the connections are negative [example (iii)]. In Fig. 3 we compare the numerical solution of Eq. (1) with our theoretical approximations in Eqs. (32) and (36) for ten realizations of the network and frequencies. We show the average of the order parameter r^2 over ten realizations of the network (triangles with thin error bars), the average of the TAT [Eq. (32), solid line with oval error bars], and the average of the FDA [Eq. (36), dashed line]. The error bar widths represent one standard deviation of the sample of ten realizations. As in the previous examples, the FDA did not show noticeable variations for different realizations of the network. We observe that the order parameter computed from our theory yields a slightly larger value than that obtained from the numerical solution of Eq. (1), but in general both the transition point and the behavior of the order parameter are described satisfactorily by the theory.

In this case, the phases ψ_n obtained from numerical solution of Eq. (32) do not depend on n, i.e., $\psi_n=\psi_m$ for all n, m. This can be understood on the basis that there are not enough negative coupling terms to make the right-hand side of Eq. (12) negative, so that a solution exists in which all the phases ψ_n are equal. As mentioned in Sec. IV, the difference in the phases in Eq. (32) prevents the right-hand side of Eq. (12) from becoming negative in the presence of negative connections. As a confirmation of this we note that as $k\to\infty$ the order parameter r appears to approach 1/3 (the dot-dashed horizontal line in Fig. 3), which corresponds to $(\psi_n-\psi_m)\to 0$ in Eq. (35) for $q=2/3$. The fact that both the phases ψ_n and θ_n do not depend on n as $k\to\infty$ is consistent with Eq. (7).

In order to consider a case in which the effect of the negative connections is more extreme, we consider a network constructed as described above with $q=0.54$ [example (iv)]. In Fig. 4 we compare the numerical solution of Eq. (1) with our theoretical approximations in Eqs. (32) and (36) for ten realizations of the network and frequencies. We show the average of the order parameter r^2 over ten realizations of the network (triangles with thin error bars), the average of the FDA [Eq. (36), dashed line with thin error bars] and the average of the TAT [Eq. (32), solid line with oval error bars].

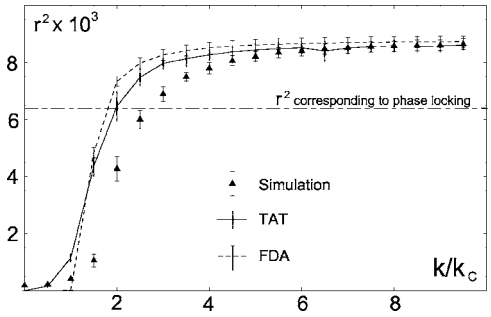

FIG. 4. Average of the order parameter r^2 obtained from numerical solution of Eq. (1) over ten realizations of the network with $q=0.54$ and frequencies (triangles) and average of the TAT (solid line) as a function of k/k_c. Note the different scale in the horizontal axis as compared with the previous figures. The horizontal dot-dashed line represents the value of the order parameter if the oscillators were phase locked ($\theta_n=\theta_m$ for all m and n).

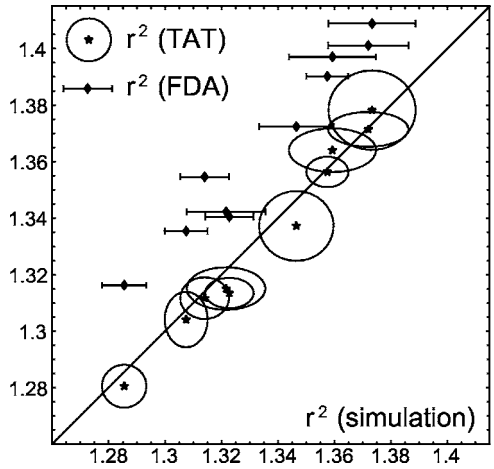

FIG. 5. Order parameter r^2 obtained from the TAT (stars surrounded by ellipses) and from the FDA (diamonds with horizontal bars) versus the value obtained from numerical solution of Eq. (1) for $k/k_c=8$. The solid line is the identity. Each point corresponds to a realization of the network, with results averaged over ten realizations of the frequencies. The ellipses and bars indicate the spread in the results for different realizations; see the text. Besides a small positive bias in the FDA, the theories track the spread in the results of the numerical solution for different realizations.

When numerically solving Eq. (32) by iteration of Eq. (33), on some occasions a period two orbit was found instead of the desired fixed point. If we denote the left hand side of Eq. (33) by z_n^{j+1} and the right hand side by $f(z_n^j)$, we found that convergence to a fixed point was facilitated by replacing the right hand side by $[z_n^j+f(z_n^j)]/2$ and finding the fixed points of this modified system.

In this example, at low coupling strengths [roughly $k/k_c \lesssim 4$, where k_c is computed from Eq. (37)] the order parameter computed from numerical solution of Eq. (1) is smaller than that obtained from the TAT and FDA. As k increases, however, the TAT and FDA theories captures the asymptotic value of the order parameter r. We note that in this case the asymptotic value is larger than that corresponding to phase locking [i.e., the one obtained by setting $\psi_n=0$ in Eq. (35), $r\approx 0.54-0.46=0.08$], which we indicate by a horizontal dot-dashed line in Fig. 4, and much smaller than $r=1$, the value corresponding to no frustration [i.e., $\psi_n-\psi_m=0$ for $A_{nm}>0$ and π for $A_{nm}<0$ in Eq. (35)]. The small scale of the horizontal axis is due to the fact that we are plotting r^2, and to our definition of the order parameter which assigns a value of 1 to a nonfrustrated configuration. The small value of the order parameter indicates a strong frustration.

We note that in this example, in contrast with the examples discussed so far, there is variation in the values of the order parameter predicted by the FDA for different realizations of the network. This indicates that, as the expected value of the coupling strengths A_{nm} becomes small (i.e., $|q-1/2|$ small), fluctuations due to the realization of the network become noticeable. Although the values predicted by the FDA and TAT depend on the realization of the network and frequencies, we note for $k/k_c \gtrsim 6$ that these values track the values observed for the numerical simulations of the corresponding realization. As an illustration of this, we plot in Fig. 5 the values of r^2 obtained from the TAT (stars) and the values of r^2 obtained from the FDA (diamonds) versus the value obtained from numerical solution of Eq. (1) for $k/k_c=8$. Each point corresponds to a given realization of the network, with results averaged over ten realizations of the frequencies. The ellipses surrounding the stars (TAT data) have vertical and horizontal half-width corresponding to the standard deviation of r^2 (TAT) and r^2 (simulation) for the ten frequency realizations. The half-width of the horizontal bars on the diamonds (FDA data) indicates the standard deviation of r^2 (simulation). Since the FDA already averages over the frequencies, all the FDA values are the same for a given realization of the network. In this Figure we can see that, besides a small positive bias in the FDA, the theories track the spread in the results of the numerical solution for different realizations. Some bias in the FDA is not surprising, because we averaged the right hand side of the nonlinear equation (12) for the TAT in order to get Eq. (13) for the FDA. Nonetheless, the bias is extremely small in most of our examples.

The behavior observed in Fig. 4 at $k/k_c \lesssim 4$ can be interpreted as a shift in the transition point to a larger value of the coupling strength, and is reminiscent of what occurs when the time fluctuations [$kh_n(t)$ in Eq. (5)] neglected in Eq. (6) have an appreciable effect.[12] We believe that the time fluctuations have a more pronounced effect as the number of negative connections becomes comparable to the number of positive connections (i.e., as $|q-\frac{1}{2}|$ becomes small) because the critical coupling strength k_c becomes large (roughly $k_c \sim |q-\frac{1}{2}|^{-1}$). In particular, with positive connections, the condition for neglecting $kh_n(t)$ was that the number of connections to each node was large. In contrast, for the present case, the analogous statement would be that $|q-1/2|$ times the number of connections is large, which is much less well satisfied, $|q-\frac{1}{2}|400=0.04\times 400=16$. The extreme case of zero mean coupling has already been studied numerically by Daido,[19] who found that in this case the oscillators lock in the sense that their average frequency is the same, but their phases diffuse. As argued in Ref. 12, such fluctuations have the effect of shifting the transition to larger values of the coupling strength. It would be interesting to carry on simu-

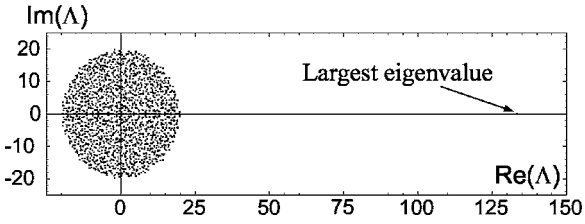

FIG. 6. Complex eigenvalues Λ (dots) of a 1500×1500 random matrix whose off diagonal entries are 1, -1 or 0 with probabilities 8/45, 4/45, and 11/15, respectively. One eigenvalue is located at $\lambda=136.2$, while the other 1499 eigenvalues uniformly fill a circle of radius ρ centered at the origin of the complex Λ plane. Note that $\rho\approx19.8$ is substantially less than 136.2. Comparing with the theory in the Appendix , Eq. (A2) yields a prediction of 133.3 for the maximum real eigenvalue while Eq. (A1) predicts 19.7 for ρ. These are in excellent agreement with our numerically determined values.

lations in networks with a much larger number of connections per node, as the effect of fluctuations would likely be reduced.

We also considered a case in which the adjacency matrix is asymmetric and has mixed positive-negative connections. For $N=1500$ nodes, we constructed an adjacency matrix by setting its nondiagonal entries to 1, -1, and 0 with probability 8/45, 4, 45, and 11/15, respectively. The latter probability yields an expected number of connections of 400. Our theories work satisfactorily in this case, and, since the results are similar to those in Fig. 3, we do not show them. In this case there is no guarantee that there is a real eigenvalue [as needed for estimating the critical coupling strength in Eq. (15)], or that the largest real eigenvalue (if there is one) has the largest real part. Numerically, we find that for matrices constructed as in this example there is a real positive eigenvalue and that, furthermore, it is well separated from the largest real part of the remaining eigenvalues (see Fig. 6). We also find this for other values of q provided $|q-\frac{1}{2}|$ is not too small. We provide a discussion of this issue and show the spectrum of the adjacency matrix in the Appendix.

VI. DISCUSSION

In this paper, we have considered interacting phase oscillators [Eq. (1)] connected by directed networks and networks with mixed positive-negative connections. We have presented theoretical approximations to the coupling strength at which a macroscopic transition to coherence takes place, and to the values of a suitably defined order parameter past the transition. In developing these approximations, one of our assumptions is that the number of connections per node is large.

The previous theory of Ref. 12 given by Eq. (12) (the time averaged theory, TAT) can still be applied for asymmetric networks with purely positive coupling and was found to give good predictions, applicable to *individual* asymmetric random realizations [Figs. 1(b) and 2(b)]. The previous theory given by Eq. (13) (the frequency distribution approximation, FDA) can also still be applied for asymmetric networks with purely positive coupling and was found to give good predictions applicable to the *ensemble average behavior* of asymmetric network realizations [Figs. 1(a) and 2(a)]. The perturbative theory for the FDA was generalized to account for directed networks [Eqs. (26) and (27)], as was the previous undirected network mean field theory, MFT [generalized from Eqs. (18)–(21) to Eqs. (28)–(31)]. In our example (ii), which had a very strong asymmetry, we found that our directed FDA perturbation theory [Eqs. (26) and (27)] gave a good description of synchronization, but that the directed mean-field approximation gave a transition to synchronization at a coupling substantially below that observed. In contrast, for example (i), in which the coupling matrices were individually asymmetric but their ensemble average was symmetric, the mean-field theory (and all the other theories in Sec. III) gave good results.

For the case of mixed positive-negative couplings we presented a generalization of the TAT and FDA, Eqs. (32)–(37). We tested these results on two examples, example (iii) in which a fraction $1-q=1/3$ of the couplings were negative, and example (iv) in which a fraction $1-q=0.46$ of the couplings were negative. For example (iii) we found that iteration of Eq. (33) converges to a fixed point with $\psi_n-\psi_m=0$, and thus the result is similar to the case where all connections are positive. In example (iv), the result of iteration of Eq. (33) yields nontrivial values for the phases ψ_n. In this case we found good agreement between the solutions of (1) and the theory for the order parameter for k/k_c large ($k/k_c\gtrsim4$), but that for smaller k/k_c ($k/k_c\lesssim4$), although yielding qualitatively similar behavior to that observed (Fig. 4), the theory overestimates the order parameter. Analogous to similar observations for symmetric networks with only positive coupling,[12] we speculate (Sec. V) that this is a finite size effect associated with the fact that the effective number of connections given in this example by $|q-\frac{1}{2}|400=16$ is not sufficiently large to justify neglect of $kh_n(t)$ in Eq. (5).

In order to isolate the effect of the asymmetry and the negative connections, we considered networks in which the degree distribution is very narrow. The combined effect of these factors with different heterogeneous degree distributions (e.g., scale free networks[21]) and with correlations in the network (in particular, degree-degree correlations) is still open to investigation.

In practice, one could be interested in networks in which the asymmetry in the connections is strongly correlated with the sign of the coupling (in analogy to some models in neuroscience[22]). Although we did not study such a case here, we believe our theory provides a good starting point to study the emergence of synchronization in these kind of structured complex networks.

ACKNOWLEDGMENTS

This work was sponsored by ONR (Physics) and by NSF (PHY 0456240).

APPENDIX: SPECTRUM OF CERTAIN RANDOM MATRICES

In this appendix we discuss the characteristics of the spectrum of the adjacency matrices considered in our examples. Although we will focus here on asymmetric matrices, a similar argument works for symmetric matrices. The matrices we consider are relatively sparse, with the position

of the nonzero entries being chosen randomly (e.g., in the symmetric case, the position of the nonzero entries is chosen when constructing the network using the configuration model), and their values being also determined randomly from a given probability distribution (e.g., 1 with probability q and -1 with probability $1-q$). Our interest is focused on the gap between the largest real eigenvalue (if there is one) and the largest real part of the other eigenvalues. In Ref. 23 the spectrum of certain large sparse matrices with average eigenvalue 0 and row sum $\Sigma_{m=1}A_{nm}=1$ was described and a heuristic analytical approach was proposed. Using results for matrices with zero mean Gaussian random entries,[24] Ref. 23 predicts that the spectrum of the non-Gaussian random matrices they consider consists of a trivial eigenvalue $\lambda=1$ with the remaining eigenvalues distributed uniformly in a circle centered at the origin of the complex plane with radius

$$\rho=\sqrt{N}\sigma, \tag{A1}$$

where σ^2 is the variance of the entries of the matrix. We find that this approach also succeeds in describing the spectrum of the matrices in our examples. In our case, the diagonal entries are 0, so that the average eigenvalue is also 0 as in Ref. 23. We find that there is always a largest real eigenvalue approximately given by the mean field value

$$\lambda=\langle\tilde{d}^2\rangle/\langle\tilde{d}\rangle \tag{A2}$$

(see Refs. 12 and 25), where $\tilde{d}_n=\Sigma_{m=1}^{N}A_{nm}$ and $\langle\tilde{d}^2\rangle=\Sigma_{n=1}^{N}\tilde{d}_n^2$, which in the case considered in Ref. 23 reduces to $\lambda=1$. We also numerically confirm that the remaining eigenvalues are uniformly distributed in a circle of radius ρ as described in Ref. 23. This is illustrated in Fig. 6.

Thus for $N\gg 1$ if $\lambda>\rho$ there is a gap of size $\lambda-\rho$ between the largest real eigenvalue and real part of the rest of the eigenvalue spectrum. Using Eqs. (A1) and (A2) it can be shown that, for networks with large enough number of connections per node or with enough positive (or negative) bias in the coupling strength, there is a wide separation between the largest eigenvalue and the largest real part of the remaining eigenvectors. For symmetric matrices, similar results apply (i.e., the bulk of the spectrum of the matrix A can be approximately obtained as described above using Wigner's semicircle law).

[1] A. Pikovsky, M. G. Rosenblum, and J. Kurths, *Synchronization: A universal concept in nonlinear sciences* (Cambridge University Press, Cambridge, 2001).
[2] E. Mosekilde, Y. Maistrenko, and D. Postnov, *Chaotic Synchronization: Applications to Living Systems* (World Scientific, Singapore, 2002).
[3] L. M. Pecora and T. L. Carroll, Phys. Rev. Lett. **80**, 2109 (1998).
[4] M. Barahona and L. M. Pecora, Phys. Rev. Lett. **89**, 054101 (2002).
[5] T. Nishikawa, A. E. Motter, Y. -C. Lai, and F. C. Hoppensteadt, Phys. Rev. Lett. **91**, 014101 (2003).
[6] A. Jadbabaie, N. Motee, and M. Barahona, *Proceedings of the American Control Conference* (ACC 2004).
[7] J. L. Rogers and L. T. Wille, Phys. Rev. E **54**, R2193 (1996); M. S. O. Massunaga and M. Bahiana, Physica D **168-169**, 136 (2002); M. Maródi, F. d'Ovidio, and T. Vicsek, Phys. Rev. E **66**, 011109 (2002).
[8] Y. Moreno and A. E. Pacheco, Europhys. Lett. **68**, 603 (2004).
[9] T. Ichinomiya, Phys. Rev. E **70**, 026116 (2004).
[10] D. -S. Lee, eprint cond-mat/0410635.
[11] T. Ichinomiya, eprint cond-mat/0507285.
[12] Juan G. Restrepo, Brian R. Hunt, and Edward Ott, Phys. Rev. E **71**, 036151 (2005).
[13] Y. Kuramoto, *Chemical Oscillations, Waves, and Turbulence* (Springer-Verlag, Berlin, 1984).
[14] S. H. Strogatz, Physica D **143**, 1 (2000).
[15] M. E. J. Newman, SIAM Rev. **45**, 167 (2003).
[16] A. -L. Barabási and R. Albert, Rev. Mod. Phys. **74**, 47 (2002).
[17] In Ref. 12 we argue, based on Ref. 10, that Eqs. (16) and (17) are valid in the limit $N\to\infty$ for degree distributions $p(\tilde{d})$ such that $\int_1^\infty p(\tilde{d})\tilde{d}^4 d\tilde{d}$ is finite.
[18] R. B. Bapat and T. E. S. Raghavan, *Nonnegative Matrices and Applications* (Cambridge University Press, Cambridge, 1997).
[19] H. Daido, Phys. Rev. Lett. **68**, 1073 (1992).
[20] T. Nishikawa, Y. -C. Lai, and F. C. Hoppensteadt, Phys. Rev. Lett. **92**, 108101 (2004).
[21] A. -L. Barabási and R. Albert, Science **286**, 509 (1999).
[22] X. -J. Wang, Neuron **36**, 955 (2002).
[23] M. Timme, F. Wolf, and T. Gheisel, Phys. Rev. Lett. **92**, 074101 (2004).
[24] H. J. Sommers, A. Crisanti, H. Sompolinsky, and Y. Stein, Phys. Rev. Lett. **60**, 1895 (1988).
[25] F. Chung, L. Lu, and V. Vu, Proc. Natl. Acad. Sci. U.S.A. **100**, 6313 (2003).